

## Imaging Anyons with Scanning Tunneling Microscopy

Zlatko Papić,<sup>1</sup> Roger S. K. Mong,<sup>2</sup> Ali Yazdani,<sup>3,\*</sup> and Michael P. Zaletel<sup>3,†</sup>

<sup>1</sup>*School of Physics and Astronomy, University of Leeds, Leeds LS2 9JT, United Kingdom*

<sup>2</sup>*Department of Physics and Astronomy, University of Pittsburgh, Pittsburgh, Pennsylvania 15260, USA*

<sup>3</sup>*Department of Physics, Princeton University, Princeton, New Jersey 08540, USA*



(Received 16 September 2017; published 6 March 2018)

Anyons are exotic quasiparticles with fractional charge that can emerge as fundamental excitations of strongly interacting topological quantum phases of matter. Unlike ordinary fermions and bosons, they may obey non-Abelian statistics—a property that would help realize fault-tolerant quantum computation. Non-Abelian anyons have long been predicted to occur in the fractional quantum Hall (FQH) phases that form in two-dimensional electron gases in the presence of a large magnetic field, such as the  $\nu = 5/2$  FQH state. However, direct experimental evidence of anyons and tests that can distinguish between Abelian and non-Abelian quantum ground states with such excitations have remained elusive. Here, we propose a new experimental approach to directly visualize the structure of interacting electronic states of FQH states with the STM. Our theoretical calculations show how spectroscopy mapping with the STM near individual impurity defects can be used to image fractional statistics in FQH states, identifying unique signatures in such measurements that can distinguish different proposed ground states. The presence of locally trapped anyons should leave distinct signatures in STM spectroscopic maps, and enables a new approach to directly detect—and perhaps ultimately manipulate—these exotic quasiparticles.

DOI: [10.1103/PhysRevX.8.011037](https://doi.org/10.1103/PhysRevX.8.011037)

Subject Areas: Condensed Matter Physics, Graphene, Strongly Correlated Materials

Unlike spontaneous symmetry breaking, which is characterized by a local order parameter, detecting topological order requires a “nonlocal” probe sensitive to the fractional phases anyons accrue when they wind around each other [1]. Detecting these phases would seem to require the construction of an “anyon interferometer” in which one test particle is controllably brought around another, as has been proposed for fractional quantum Hall (FQH) systems [2–4]. But in fact, spectroscopy—even an atomically local one like STM—is inherently nonlocal: accurately resolving energies detects properties of quasiparticles separated by long times. Previous proposals for topological spectroscopy include the tunneling conductance of FQH edge states [5], the threshold behavior of neutron scattering in spin liquids [6], and the structure of rf absorption lines of trapped cold-atomic FQH droplets [7]. These experiments could narrow down the nature of the topological order, though they could not be used to image the presence of individual anyons localized in the bulk.

Until recently, STM in the bulk of a FQH state was largely impractical, since the pristine two-dimensional electron gases (2DEGs) required were only possible to realize in quantum wells sandwiched deep between semiconductors (though workarounds have been proposed [8,9]). The observation of QH effects in graphene [10] and the surface states of bismuth [11], where the 2DEG can be made atomically close to the vacuum, removes this obstacle. In these systems, STM has been able to detect the single-particle quantization which gives rise to the integer quantum Hall effect (IQHE), as well as interaction-induced exchange gaps which result in quantum Hall ferromagnetism [12–15]. More relevant to our studies here, recent experiments have found that when the samples contain very few defects (a single defect within several magnetic lengths), STM can directly probe the spatial structure of the Landau orbits, and further use this capability to visualize when the ground state breaks the symmetry of the underlying lattice [15]. In bilayer graphene, a putative non-Abelian even-denominator state is observed in suspended and encapsulated samples [16–18]. In the open-faced samples potentially amenable to STM a plethora of robust FQH states are observed [19], though not yet the even-denominator state. These advances make examining the prospects for STM studies in the fractional regime a timely topic.

What could STM spectroscopy and its ability to make spatially resolved measurement reveal about the nature of

\*yazdani@princeton.edu

†mzaletel@princeton.edu

Published by the American Physical Society under the terms of the [Creative Commons Attribution 4.0 International license](https://creativecommons.org/licenses/by/4.0/). Further distribution of this work must maintain attribution to the author(s) and the published article's title, journal citation, and DOI.

topological excitations in the FQH effect? Assuming that STM as a function of the bias  $E = eV$  at a location  $\mathbf{r}$  measures the local density of states (LDOS), i.e., the differential conductance  $[(dI)/dV](\mathbf{r}) \propto \text{LDOS}(eV, \mathbf{r})$ , then in the bulk of a perfectly clean insulating QH system such measurements should simply show a charging gap and would be spatially featureless. Approaching the edges the behavior of the spectra would change, where in contrast to the bulk, tunneling spectra should show power-law energy dependence  $E^g$  [5]. So naively, besides the potential for edge spectroscopy one might expect that local STM measurements would not be a useful tool to study anyons in the bulk of a FQH phase.

The key insight, however, is to consider the FQH phases when there is a single isolated impurity (e.g., a lattice defect or a pinned charge) and examine the LDOS on the length scale of the magnetic length surrounding this impurity. As we demonstrate here, the LDOS develops spatial modulations near the impurity due to the rich spectrum of discrete bound states. An electron injected by the STM splits into  $q$  charge  $-e/q$  anyons, so the local STM spectrum should be interpreted as the distinct energies at which  $q$  anyons can be bound to the impurity [20]. Remarkably, we find that the counting of the impurity bounded levels is sensitive to the “fractional exclusion statistics” of anyons, which as first considered by Haldane [7,21,22] interpolates between the statistics of bosons and fermions. Using both model wave function calculations and numerical exact diagonalization studies, we find that the local spectrum can be a powerful new method to detect underlying topological order in the system, as different Abelian and non-Abelian phases have their own distinct spectrum near the impurity. More importantly, whether the impurity binds an anyon or not also modifies the local spectrum, thereby making it possible to use the STM as a true “anyon microscope” which can detect anyons regardless of their electrical charge (see, for example, Ref. [23] for a charge sensitive approach). We explore how these ideas may be implemented in experiments on graphene by considering realistic Coulomb interactions and impurities relevant to this system.

*Hamiltonian and LDOS.*—We begin with a description of the FQH setup illustrated in Fig. 1. We consider a 2DEG at a distance  $d_g$  above a metallic gate in a quantizing magnetic field  $B$ , as realized, for example, in a graphite on boron-nitride on graphene heterostructure. Because of the image charges induced by the gate [24,25], the Coulomb interaction between electrons in the 2DEG is screened and takes the form

$$V_C(r) = \frac{1}{r} - \frac{1}{\sqrt{(2d_g)^2 + r^2}}, \quad (1)$$

which falls off as  $r^{-3}$  for  $r \gg d_g$ . In addition, we assume an impurity with charge  $Z$  is located a distance  $d_i < d_g$

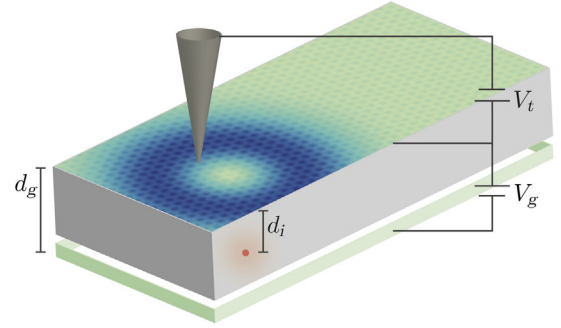


FIG. 1. Experimental setup. A metallic gate (bottom) is separated by an insulating barrier of thickness  $d_g$  from a 2DEG (top). An impurity of charge  $Z$  is located inside the barrier at distance  $d_i$  from the 2DEG. Tuning the gate voltage  $V_g$  to enter into a quantum Hall state, STM spectroscopy is used to measure the local density of states (LDOS), shown as a density plot. The LDOS will reveal a discrete set of ringlike resonances centered on the impurity, whose radius depends on the energy. By counting the number of resonances of a given radius, it is argued that the location and fractional exclusion statistics of the anyons can be determined.

below the origin of the 2DEG, leading to a one-body potential:

$$U(r) = \frac{Z}{\sqrt{d_i^2 + r^2}} - \frac{Z}{\sqrt{(2d_g - d_i)^2 + r^2}}. \quad (2)$$

In the case of graphene devices, such impurities can arise from substitutions in the boron nitride [26]. Below, we set  $Z = \pm 1$  and treat  $d_i$  as a tunable parameter.

In a strong perpendicular magnetic field  $B$ , the kinetic energy is quenched and topological phases, such as Laughlin [27] and composite fermion states [28], emerge as ground states of  $V_C$  at particular filling fractions  $\nu = N/N_\phi$ , where  $N$  is the number of electrons and  $N_\phi$  is the magnetic flux piercing the 2DEG. The states that appear are insensitive to  $d_g$  once  $d_g \gg \ell_B$ , where  $\ell_B = \sqrt{\hbar/eB}$  is the magnetic length, so below, we fix  $d_g = 4\ell_B$ .

We begin by ignoring any influence of the tip on the measurement, where STM  $[(dI)/dV]$  spectra at positive tip bias relative to the sample is proportional to the occupied LDOS:

$$\text{LDOS}(E = eV, \mathbf{r}) = \sum_a \delta(E - E_a) |\langle a | \hat{\psi}(\mathbf{r}) | \Omega \rangle|^2. \quad (3)$$

Here,  $|\Omega\rangle$  is the ground state,  $\hat{\psi}(\mathbf{r})$  is the electron destruction operator, and  $|a\rangle$  runs over all excited states with one less electron than  $\Omega$ . The energy  $E_a$  of the excited state is measured relative to the difference in work function between the ground state of the sample and the tip, a point we will return to. An analogous expression holds for the unoccupied LDOS with  $\hat{\psi} \rightarrow \hat{\psi}^\dagger$ . Because quantum Hall

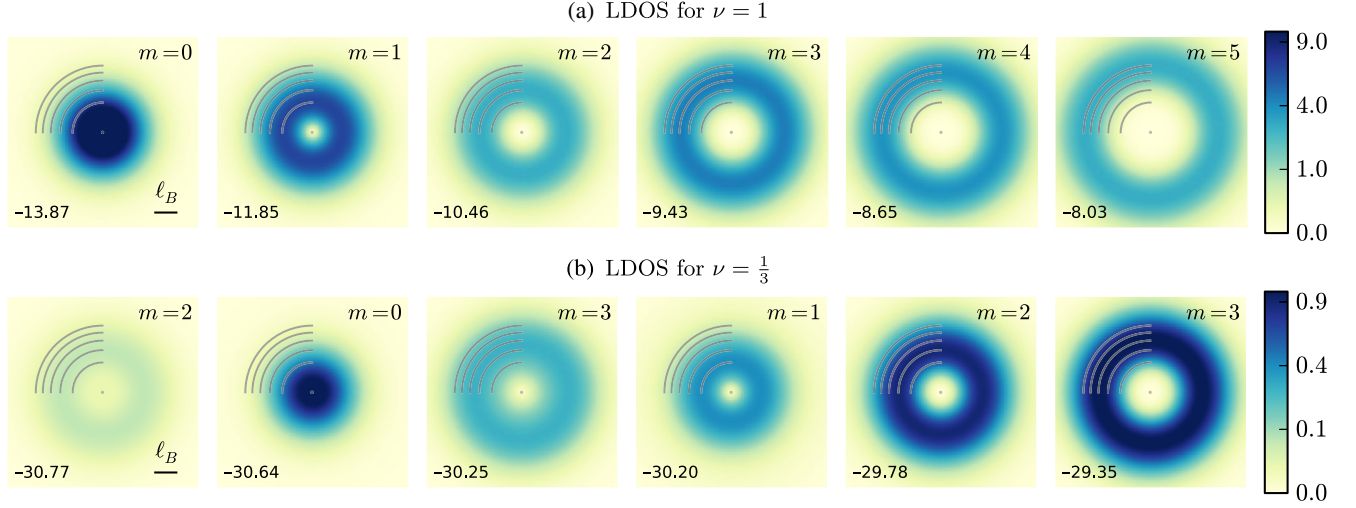


FIG. 2. The simulated occupied LDOS( $E, \mathbf{r} = x, y$ ) for the  $\nu = 1$  IQHE and  $\nu = 1/3$  Laughlin phase. The calculations assume a dipolar Coulomb interaction [Eq. (1)] and charged impurity located below the origin [Eq. (2)]. Each image is at a fixed  $E$  annotated in the lower left in units of meV at  $B = 14$  T, and a scale bar indicates  $\ell_B \sim 7$  nm. Away from the displayed  $E$ , there is no DOS. The white arcs denote the density maxima  $r_m$  of the  $m$ th single-particle orbital. (a) For  $\nu = 1$ , each orbital lights up once while sweeping through the energy, indicating there is a single hole excitation for each angular momentum  $m$ . The impurity has charge  $e$  and is situated at  $d_i = 3.1\ell_B$  below the 2DEG. (b) For  $\nu = 1/3$ , the  $m = 2$  ring lights up *twice*, once at energy  $-30.77$  meV, and once again at  $-29.78$  meV. This indicates there are multiple many-body excitations associated with removing an electron from orbital  $m$ , as a result of strong correlations. The system contains  $N_\phi = 24$  flux quanta with impurity at  $d_i = 2.7\ell_B$ .

states are gapped, a finite bias is required before any tunneling occurs.

The Hamiltonian is strongly interacting, so to compute the LDOS exactly we must resort to numerical diagonalization of a finite number of electrons on a sphere, where the bulk properties can be conveniently probed without edge effects [29,30] (see Supplementary Materials [31]). In Fig. 2, we show the resulting prediction for the occupied LDOS near the impurity, both for the IQHE ( $\nu = 1$ ) and the Laughlin phase ( $\nu = \frac{1}{3}$ ). The LDOS reveals a discrete set of ringlike features centered around the impurity whose radius and intensity depends on the energy.

To understand the ring features in the LDOS, we turn to the single-particle physics of the Landau level (LL). In strong magnetic fields, the many-electron system can be modeled in a restricted Hilbert space of the given LL [34]. In the lowest LL relevant to fillings  $\nu = \frac{1}{3}$  and 1, the single-electron states on the plane (in the symmetric gauge) are given by

$$\phi_m(\mathbf{r}) \propto r^m e^{i\phi m} e^{-r^2/(4\ell_B^2)}, \quad m = 0, 1, 2, \dots, \quad (4)$$

where  $(r, \phi)$  are polar coordinates. Notably, their density,  $|\phi_m(\mathbf{r})|^2$ , is concentrated in rings of radii  $r_m = \sqrt{2m}\ell_B$  around the impurity. To good approximation, the Hamiltonian of the 2DEG then consists of potentials  $V_C(r)$  and  $U(r)$  projected into the many-body Hilbert space of the lowest LL.

To compute the LDOS at energies small compared to the cyclotron gap between LLs, the electron operator can be

expanded as  $\hat{\psi}(\mathbf{r}) = \sum_m \phi_m(\mathbf{r}) \hat{c}_m$ , where  $\hat{c}_m$  removes an electron from orbital  $m$ . If we further assume that the impurity potential is rotationally symmetric on the scale of  $\ell_B$ , so that the angular momentum  $L^z = \hbar m$  is a good quantum number, we can insert this expansion into Eq. (3) to obtain

$$\text{LDOS}(E, \mathbf{r}) = \sum_a \delta(E - E_a) |\phi_{m_a}(r)|^2 |\langle a | c_{m_a} | \Omega \rangle|^2, \quad (5)$$

where  $\hbar m_a$  is the angular momentum of excited state  $a$ . The rings that appear in the LDOS thus arise because each excited state  $a$  contributes to the LDOS only around a ring  $|\phi_{m_a}(r)|^2$  of radius  $r_{m_a}$ .

The ring structures in the LDOS at high magnetic field allows us to convert the real-space information into an angular momentum  $m$  [35], so STM can be thought of as  $L^z$  resolved (at least for low  $m$ —the inverse problem becomes ill-conditioned for large  $m$ , where the  $r_m = \sqrt{2m}\ell_B$  become too closely spaced compared with  $\ell_B$  to accurately assign). Thus, rather than plotting the LDOS in real space, it is more compact to plot the intensity in the  $m$ th ring,

$$\text{LDOS}(E, m) = \sum_a \delta(E - E_a) |\langle a | \hat{c}_m | \Omega \rangle|^2, \quad (6)$$

as shown in Fig. 3. It reveals a set of energies that disperse with  $m$ .

**IQHE.**—This dispersion is easiest to understand at  $\nu = 1$  [36], shown in Fig. 3(a). The ground state  $|\Omega\rangle$  is a full LL,

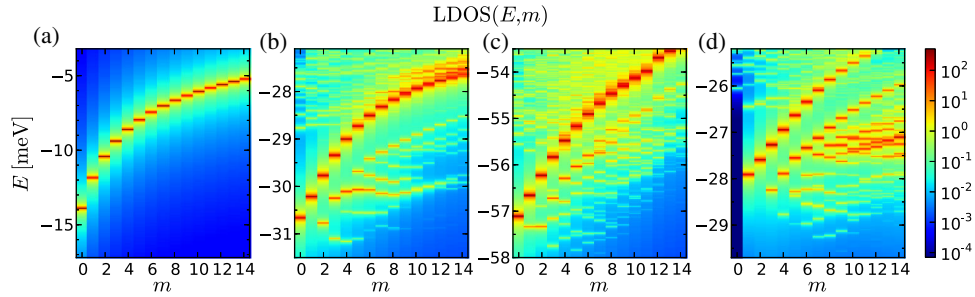


FIG. 3. The orbital-resolved LDOS( $E, m$ ) for various states. In all cases a phenomenological width of  $7 \mu\text{eV}$  was added to the data. (a) The IQH state. There is one level for each  $m$ . (b) The  $\nu = 1/3$  FQH state, with no anyons localized on the impurity. There are now multiple energy levels for each  $m$ . The counting of the low-lying levels (i.e., the number of excitations at each  $m$ ) is  $1, 1, 2, 3, 4, 5, \dots$ . States above the brightest band form a nonuniversal continuum. (c) The  $\nu = 5/2$  Moore-Read state. The counting of the low-lying levels is  $1, 2, 3, 5, \dots$ . In order to break particle-hole symmetry, a small component of three-body interaction  $V_{3b} = 0.1$  was added to the screened Coulomb Hamiltonian. The system contains  $N_\phi = 25$  flux quanta with impurity at  $d_i = 2.3\ell_B$ . (d) Same as (b) but in the presence of a charge- $e/3$  anyon bound to the impurity. The counting of the low-lying levels is now  $0, 1, 1, 2, 3, \dots$ . The system contains  $N_\phi = 24$  flux quanta with impurity at  $d_i = 2.8\ell_B$ .

while the excited states  $a$  consist of a hole in orbital  $m = a$ ,  $|a\rangle = c_a|\Omega\rangle$ . The impurity potential decomposes into the energies for occupying each orbital:  $\hat{U} = \sum_{m=0}^{\infty} U_m \hat{n}_m$ , where  $U_m \sim U(r_m)$  characterizes the radial falloff of the impurity potential. Thus, the tunneling DOS into orbital  $m$  is shifted down in energy by  $U_m$  relative to the region far from the impurity. There is one state per  $m$ ; i.e., the “counting” is  $1, 1, 1, \dots$  (inter-LL excitations, which we ignore, occur at a much higher energy).

STM experiments have already shown that such impurity-induced shifts of the orbital levels near single impurities can be resolved experimentally in the IQHE case. In the case of a graphene on boron-nitride heterostructure, spectroscopic measurements near individual impurity could resolve levels corresponding to  $m = 0, 1, 2$  orbitals of the  $N = 0$  LL, while higher  $m$  appeared as a continuum [14]. In studies of Bi surface states at high magnetic fields [15], atomic-sized impurities were found to shift the  $L^z = 0$  orbital in each of the  $N$ th LL (for both electron and holelike LL), and could not only be detected in energy-resolved experiments but also spatially mapped with high resolution. The latter experiments demonstrate that in samples with low defect density (less than one per magnetic length), STM spectroscopic maps are capable of resolving features such as those in Fig. 3(a).

*Fractional phases.*—We now examine how the structure of the LDOS near impurities differs between integer and fractional cases. The  $\nu = \frac{1}{3}$  case, Fig. 3(b), demonstrates this difference by showing that rather than one state per  $m$ , most of the  $m$  have *multiple* energies appearing in the LDOS. Although some of these states belong to a high-energy continuum, there is also a band of discrete low-energy levels whose number grows with angular momentum  $m$  as  $1, 1, 2, 3, 4, 5, 7, \dots$ . This multiplicity is a result of fractionalization. When an electron is removed from the Laughlin state, the hole fractionalizes into three

independent charge  $e/3$  quasiholes [27]. Because they can have motion relative to each other, there are multiple three-quasihole states of a given total angular momentum  $\hbar m$ . The quasiholes have a “topological interaction,” their fractional statistics, which results in a  $2\pi/3$  Berry phase whenever one winds around another. The fractional statistics change the angular momentum, and hence counting, of the three-quasihole states. Note there is no “orthogonality catastrophe” in this situation, since almost the entirety of the spectral weight lies in this discrete set of low-energy states: while the lower-energy charge  $e/3$  excitation is orthogonal to the electron, the electron itself is readily reconstructed from three of them [37].

More generally, in a FQH phase where the hole splits into  $q$  charge  $e/q$  anyons, the orbitally resolved LDOS reveals all the distinct eigenstates in which the  $q$  anyons have total angular momentum  $\hbar m$ . While we do not know how to compute this counting in complete generality, for many FQH states the observed sequence can be predicted using “ $(k, r)$  fractional exclusion statistics” [21,38], as explained in Table I. The same insight was used to predict the rf spectroscopy of small bosonic FQH droplets, which also proved sensitive to the  $(k, r)$  statistics [7]. All FQH phases captured by one (or more)  $(k, r)$  rule, including the Laughlin and  $\mathbb{Z}_k$  Read-Rezayi sequences, have distinct LDOS counting sequences. For example, the non-Abelian Moore-Read state [39], whose LDOS we show in Fig. 3(c), is predicted by Table I to have counting  $1, 2, 3, 5, \dots$ . The “ $k$ ” of a  $(k, r)$  state can be determined from the counting of the first  $m \leq k$  orbitals, and any state found to have  $k > 1$  is non-Abelian. In this sense the impurity LDOS provides a “fingerprint” for identifying the underlying topological order. Note that this counting is not the same as the counting of the edge excitations, though it is closely related to the counting of the “particle entanglement spectrum,” which has been used to numerically identify FQH phases [40].

TABLE I. Computing the LDOS counting of the Laughlin and Moore-Read state. The low-energy states of many FQH phases can be captured by their “root configuration,” which serves as a representative cartoon of the many-body wave function. Each root configuration represents a state  $|n_0, n_1, \dots\rangle$  specifying the electron occupation  $n_m$  of orbital  $m$ . Here, every row is a root configuration with the empty (filled) orbitals denoted by  $\cdot$  ( $\bullet$ ) symbols. The low-energy root configurations of a FQH phase satisfy a “ $(k, r)$  exclusion rule” [38]. The  $\nu = 1/3$  Laughlin phase satisfies the (1,3) rule: there is at most 1 particle in every 3 consecutive orbitals. The Moore-Read phase satisfies the (2,4) rule: no more than 2 particles within 4 neighboring orbitals. In each case, the ground state  $|\Omega\rangle$  corresponds to the densest configuration of particles obeying the exclusion rule. The low-energy charge  $e$  states are enumerated by root configurations with one less particle than  $|\Omega\rangle$  which *still* obey the  $(k, r)$  rule. As the angular momentum is  $L^z = \hbar \sum_m m n_m$ , we can compute the angular momentum of the charge  $e$  states relative to the ground state, which is denoted in the first column. The number of possible configurations of a given angular momentum (1, 1, 2, 3, etc. for the Laughlin and 1, 2, 3, 5, etc. for the Moore-Read) is the counting of the LDOS. In the case of the  $1/3$  phase, the root configuration in the presence of a trapped quasihole,  $|e/3\rangle$ , is obtained by shifting  $\Omega$  outwards by one.

Laughlin										Moore-Read												
$m$	0	1	2	3	4	5	6	7	8	9	$m$	0	1	2	3	4	5	6	7	8	9	...
$ \Omega\rangle$	$\bullet$	$\cdot$	$\cdot$	$\cdot$	$\cdot$	$\cdot$	$\cdot$	$\cdot$	$\cdot$	$\cdot$	$ \Omega\rangle$	$\bullet$	$\bullet$	$\cdot$	$\cdot$	$\cdot$	$\cdot$	$\cdot$	$\cdot$	$\cdot$	$\cdot$	$\cdot$
0	$\cdot$	$\cdot$	$\cdot$	$\cdot$	$\cdot$	$\cdot$	$\cdot$	$\cdot$	$\cdot$	$\cdot$	0	$\cdot$	$\cdot$	$\cdot$	$\cdot$	$\cdot$	$\cdot$	$\cdot$	$\cdot$	$\cdot$	$\cdot$	$\cdot$
1	$\cdot$	$\cdot$	$\bullet$	$\cdot$	1	$\bullet$	$\cdot$	$\cdot$	$\cdot$	$\cdot$	$\cdot$	$\cdot$	$\cdot$	$\cdot$	$\cdot$	$\cdot$						
2	$\cdot$	$\bullet$	$\cdot$	$\cdot$	$\cdot$	$\cdot$	$\cdot$	$\cdot$	$\cdot$	$\cdot$	2	$\cdot$	$\bullet$	$\cdot$	$\cdot$	$\cdot$	$\cdot$	$\cdot$	$\cdot$	$\cdot$	$\cdot$	$\cdot$
3	$\bullet$	$\cdot$	$\cdot$	$\cdot$	$\cdot$	$\cdot$	$\cdot$	$\cdot$	$\cdot$	$\cdot$	3	$\cdot$	$\bullet$	$\cdot$	$\cdot$	$\cdot$	$\cdot$	$\cdot$	$\cdot$	$\cdot$	$\cdot$	$\cdot$
	$\cdot$	$\cdot$	$\cdot$	$\cdot$	$\cdot$	$\cdot$	$\cdot$	$\cdot$	$\cdot$	$\cdot$		$\cdot$	$\cdot$	$\bullet$	$\cdot$	$\cdot$	$\cdot$	$\cdot$	$\cdot$	$\cdot$	$\cdot$	$\cdot$
	$\cdot$	$\cdot$	$\cdot$	$\cdot$	$\cdot$	$\cdot$	$\cdot$	$\cdot$	$\cdot$	$\cdot$		$\cdot$	$\cdot$	$\cdot$	$\bullet$	$\cdot$	$\cdot$	$\cdot$	$\cdot$	$\cdot$	$\cdot$	$\cdot$
	$\cdot$	$\cdot$	$\cdot$	$\cdot$	$\cdot$	$\cdot$	$\cdot$	$\cdot$	$\cdot$	$\cdot$		$\cdot$	$\cdot$	$\cdot$	$\cdot$	$\bullet$	$\cdot$	$\cdot$	$\cdot$	$\cdot$	$\cdot$	$\cdot$
Laughlin + $e/3$ hole												$\cdot$	$\cdot$	$\cdot$	$\cdot$	$\cdot$	$\cdot$	$\cdot$	$\cdot$	$\cdot$	$\cdot$	$\cdot$
$ \frac{e}{3}\rangle$	$\cdot$	$\bullet$	$\cdot$	$\cdot$	$\cdot$	$\cdot$	$\cdot$	$\cdot$	$\cdot$	$\cdot$		$\cdot$	$\cdot$	$\cdot$	$\cdot$	$\cdot$	$\cdot$	$\cdot$	$\cdot$	$\cdot$	$\cdot$	$\cdot$
1	$\cdot$	$\cdot$	$\cdot$	$\cdot$	$\cdot$	$\cdot$	$\cdot$	$\cdot$	$\cdot$	$\cdot$		$\cdot$	$\cdot$	$\cdot$	$\cdot$	$\cdot$	$\cdot$	$\cdot$	$\cdot$	$\cdot$	$\cdot$	$\cdot$
2	$\cdot$	$\cdot$	$\cdot$	$\cdot$	$\cdot$	$\cdot$	$\cdot$	$\cdot$	$\cdot$	$\cdot$		$\cdot$	$\cdot$	$\cdot$	$\cdot$	$\cdot$	$\cdot$	$\cdot$	$\cdot$	$\cdot$	$\cdot$	$\cdot$

We now discuss some variants of this result. From a topological perspective, an electron and hole are equivalent. Nevertheless, the unoccupied LDOS (which encodes  $|\langle a | \hat{c}_m^\dagger | \Omega \rangle|^2$ ) has a different counting than the occupied side. While this counting cannot be computed from the simplest version of the  $(k, r)$  rule, for FQH states belonging to the Jain sequence it can be predicted by appealing to the composite fermion picture [28]. For  $\nu = \frac{1}{3}$ , our numerics agree with the predicted electron counting 0, 0, 0, 1, 1, 2, 3, 4, ... in the lowest band of states, which is shifted to larger  $m$  relative to the occupied side [31]. The spectral weight of this band is small ( $\sim 10^{-3}$ ) but appears to remain finite in the thermodynamic limit.

The difference between the occupied and unoccupied LDOS could provide a valuable probe of the half-filled

Landau level, where it has proved difficult to experimentally distinguish between the Pfaffian [39], anti-Pfaffian [41,42], and particle-hole (PH) symmetric Pfaffian [43] phases, as their simplest signatures, the Hall conductance and quasiparticle charge, are identical, so more-involved experiments such as the quasiparticle tunneling conductance are required [44]. These states are the leading theoretical candidates for the half-filled plateaus of GaAs [45] and bilayer graphene [16–18]. At half filling, the system has an approximate PH symmetry which relates filled and empty orbitals of the valence LL. The occupied and unoccupied LDOS are related by PH symmetry, so any difference between them at half filling provides a sharp probe of PH-symmetry breaking. The Pfaffian and anti-Pfaffian states are particle-hole conjugates of each other (and hence break PH), while the PH Pfaffian is PH symmetric. If the counting of the LDOS on the occupied and unoccupied side are found to be identical, this is strong evidence for the PH Pfaffian (whose counting has not been predicted). On the other hand, the Pfaffian occupied counting (1, 2, 3, 5, ...) will differ from its unoccupied counting; while we are unable to calculate the latter in full, earlier calculations [46–48] suggest counting 1, 0, ... The anti-Pfaffian is analogous but with the role of occupied and unoccupied reversed. Thus, observing occupied counting 1, 2, ... would be strong evidence for the Pfaffian, and vice versa.

In the calculations thus far, the impurity was weak enough that it did not trap a charge in the ground state. However, at an electron density slightly away from the center of the plateau, there will be a finite density of quasiparticles pinned by the disorder. A quasiparticle localized on the impurity will leave its imprint on the allowed quasihole states injected by the STM, since they experience a statistical interaction. In Fig. 3(d), we show the  $\nu = \frac{1}{3}$  hole LDOS in the presence of a trapped  $e/3$  quasihole. We find distinct counting 0, 1, 1, 2, 3, 5, 6, ..., as derived from  $(k, r)$  statistics in Table I. Most strikingly, there is a complete absence of tunneling from the  $m = 0$  orbital, providing a discrete signature of the fractionalized quasiparticle which can be directly observed in STM. The LDOS near the trapped quasiparticles of the Pfaffian phase also prove to be distinct—for example, the Majorana-like charge- $e/4$  quasihole has counting 1, 2, 3, 6, ... [31]. Thus, the LDOS can be used to image the anyon type localized to each impurity.

*Experimental considerations.*—As described earlier, STM experiments on the IQHE have already observed how impurities can shift individual orbitals within a LL [14,15], and hence they support our proposal for similar STM experiments that can detect anyons and their statistics in the FQH state. However, the previous experiments and their extensions to the FQH state, for example, on high-quality graphene devices, still raise several experimental issues. We identify three potential experimental challenges

that need to be addressed: (1) tip-induced band bending, (2) charging and lifetime effects, and (3) tip-induced screening of the electron-electron interactions that give rise to FQH states.

Typically the work function of the STM tip is different than that of the sample, and as a result there is an effective electric field present in the junction beyond that due to the tip-sample voltage bias. In the case of semiconducting samples, this difference combined with poor dielectric screening results in band bending underneath the tip. Ideally, the experiments we propose here on states with poor screening can be carried out with tips that have a work function matching the sample: for graphene, graphite or carbon coated tips, or perhaps transition metal tips that have been *in situ* prepared with growth of a graphene monolayer on their surface. So far, there has not been substantial effort in engineering STM tips for this purpose.

Alternatively, a 100–200-nm-long carbon nanotube can be affixed to an otherwise blunt tip [49]. In this geometry, the work function of the blunt tip can be locally compensated by the backgate in order to achieve the desired electron filling within a large radius around the nanotube tip—simple electrostatic calculations show that the band bending at the sample can be reduced to a couple percent of the work function mismatch [31]. The work function of the nanotube may perhaps be further engineered via the magnetic flux through the tip, which introduces a minigap [50]. If nanotubes are chosen with a diameter comparable to the magnetic length, it may even be possible to use the tip itself as the impurity, with the  $m$  selectivity obtained through  $B$ -dependent matching between  $r_m$  and the radius of the nanotube.

Another natural concern is whether charging effects could complicate the proposed experiments, since we are proposing tunneling into the localized states of a QH insulator. Previous studies of impurity-shifted LL orbital states in graphene and Bi [14,15] do not appear to suffer from this problem, most likely because they are carried out in the regime where the tunneling rates (with pico- or nanoamp currents) are smaller than the inverse lifetime of the localized states that are probed. In our proposal, we would like the broadening to be large enough so that charging is not an issue, but not too large to wash out the fine structure in our spectrum. Since a nA tunneling current corresponds to a 100 ps lifetime, while the features are split on the order of 10 ps, this constraint should be possible to satisfy experimentally. The constraint can be verified by checking for linear response between the current and tunneling matrix element, as done for Shiba bound states of a superconductor [51]. An alternative spectroscopy, using planar tunnel junctions, has also made progress in circumventing charging issues [52–55]. However, while an in-plane magnetic field can be used to provide momentum resolution, it is unclear whether these spectral functions

encode any analog of the discrete, topological, counting discussed here.

Finally, another potential concern is the strength of the screening of the in-plane interactions within the 2D sample, critical to forming the FQH state, by electrons in the tip. For a nanotube on tip, the blunt tip is much farther from the sample than  $\ell_B$  (and the metallic backgate), so will not significantly affect the screening. The nanotube may contribute to screening somewhat, but it has low dimension and density of states; it would be useful to model its effect in future work [50].

In conclusion, we show that the structure of energy levels in the LDOS near an impurity encodes a sequence of integers which identifies the underlying FQH phase. When anyonic particles are localized on the impurity, the sequence changes in a unique way, making the LDOS a real-space “image” of the location of anyons. This new technique to study anyons can provide a new tool for exploring their use in topological quantum computing. For instance, it can be used to detect the presence of neutral anyons, which is necessary for measuring the outcome of non-Abelian braiding operations. While using STM spectroscopy to measure the LDOS in the FQH regime remains an open challenge, recent advances in the fabrication of graphene on boron-nitride heterostructures, and the successful application of STM to the IQHE, suggests this is a challenge worth undertaking.

Our work also raises a number of theoretical questions. For certain phases, such as the recently proposed PH Pfaffian [43], we do not know how to compute the counting of the LDOS, and we hope this work will motivate future calculations. Furthermore, while the general mathematical structure of braiding and statistics in anyon phases is well understood, how this structure relates to fractional exclusion statistics—probed here through the dimension of the several-anyon Hilbert space—is not. The relation between exchange statistics and exclusion statistics was understood for the simplest quantum Hall phases two decades ago, but deserves renewed attention in light of our recent understanding of the interplay of symmetry and topological order [56]. A full understanding of fractional exclusion statistics would prove invaluable not just for predicting the LDOS, but for spectroscopic probes of topological order more generally.

We thank B. A. Bernevig, F. D. M. Haldane, C. Laumann, S. Simon, and A. F. Young for helpful discussions. M. P. Z. and A. Y. also acknowledge the hospitality of the Aspen Center for Physics, which is supported by National Science Foundation Grant No. PHY-1607611. A. Y. acknowledges support from Gordon and Betty Moore Foundation as part of EPiQS initiative (GBMF4530), NSF-MRSEC programs through the Princeton Center for Complex Materials DMR-142054, and NSF-DMR-1608848. Z. P. acknowledges support by EPSRC Grant

No. EP/P009409/1. In compliance with EPSRC policy framework on research data, this publication is theoretical work that does not require supporting research data.

- 
- [1] D. Arovas, J.R. Schrieffer, and F. Wilczek, *Fractional Statistics and the Quantum Hall Effect*, *Phys. Rev. Lett.* **53**, 722 (1984).
- [2] C. de C. Chamon, D. E. Freed, S. A. Kivelson, S. L. Sondhi, and X. G. Wen, *Two Point-Contact Interferometer for Quantum Hall Systems*, *Phys. Rev. B* **55**, 2331 (1997).
- [3] P. Bonderson, K. Shtengel, and J. K. Slingerland, *Interferometry of Non-Abelian Anyons*, *Ann. Phys. (Amsterdam)* **323**, 2709 (2008).
- [4] R. L. Willett, *The Quantum Hall Effect at 5/2 Filling Factor*, *Rep. Prog. Phys.* **76**, 076501 (2013).
- [5] A. M. Chang, *Chiral Luttinger Liquids at the Fractional Quantum Hall Edge*, *Rev. Mod. Phys.* **75**, 1449 (2003).
- [6] S. C. Morampudi, A. M. Turner, F. Pollmann, and F. Wilczek, *Statistics of Fractionalized Excitations through Threshold Spectroscopy*, *Phys. Rev. Lett.* **118**, 227201 (2017).
- [7] N. R. Cooper and S. H. Simon, *Signatures of Fractional Exclusion Statistics in the Spectroscopy of Quantum Hall Droplets*, *Phys. Rev. Lett.* **114**, 106802 (2015).
- [8] A. Sciambi, M. Pelliccione, S. R. Bank, A. C. Gossard, and D. Goldhaber-Gordon, *Virtual Scanning Tunneling Microscopy: A Local Spectroscopic Probe of Two-Dimensional Electron Systems*, *Appl. Phys. Lett.* **97**, 132103 (2010).
- [9] M. Pelliccione, J. Bartel, A. Sciambi, L. N. Pfeiffer, K. W. West, and D. Goldhaber-Gordon, *Local Imaging of High Mobility Two-Dimensional Electron Systems with Virtual Scanning Tunneling Microscopy*, *Appl. Phys. Lett.* **105**, 181603 (2014).
- [10] Y. Zhang, Y.-W. Tan, H. L. Stormer, and P. Kim, *Experimental Observation of the Quantum Hall Effect and Berry's Phase in Graphene*, *Nature (London)* **438**, 201 (2005).
- [11] Ph. Hofmann, *The Surfaces of Bismuth: Structural and Electronic Properties*, *Prog. Surf. Sci.* **81**, 191 (2006).
- [12] Y. J. Song, A. F. Otte, Y. Kuk, Y. Hu, D. B. Torrance, P. N. First, W. A. de Heer, H. Min, S. Adam, M. D. Stiles *et al.*, *High-Resolution Tunnelling Spectroscopy of a Graphene Quartet*, *Nature (London)* **467**, 185 (2010).
- [13] D. L. Miller, K. D. Kubista, G. M. Rutter, M. Ruan, W. A. De Heer, M. Kindermann, P. N. First, and J. A. Stroscio, *Real-Space Mapping of Magnetically Quantized Graphene States*, *Nat. Phys.* **6**, 811 (2010).
- [14] A. Luican-Mayer, M. Kharitonov, G. Li, C.-P. Lu, I. Skachko, and A.-M. B. Gonçalves, K. Watanabe, T. Taniguchi, and E. Y. Andrei, *Screening Charged Impurities and Lifting the Orbital Degeneracy in Graphene by Populating Landau Levels*, *Phys. Rev. Lett.* **112**, 036804 (2014).
- [15] B. E. Feldman, M. T. Randeria, A. Gyenis, F. Wu, H. Ji, R. J. Cava, A. H. MacDonald, and A. Yazdani, *Observation of a Nematic Quantum Hall Liquid on the Surface of Bismuth*, *Science* **354**, 316 (2016).
- [16] D.-K. Ki, V. I. Fal'ko, D. A. Abanin, and A. F. Morpurgo, *Observation of Even Denominator Fractional Quantum Hall Effect in Suspended Bilayer Graphene*, *Nano Lett.* **14**, 2135 (2014).
- [17] A. A. Zibrov, C. Kometter, H. Zhou, E. M. Spanton, T. Taniguchi, K. Watanabe, M. P. Zaletel, and A. F. Young, *Tunable Interacting Composite Fermion Phases in a Half-Filled Bilayer-Graphene Landau Level*, *Nature (London)* **549**, 360 (2017).
- [18] J. I. A. Li, C. Tan, S. Chen, Y. Zeng, T. Taniguchi, K. Watanabe, J. Hone, and C. R. Dean, *Even Denominator Fractional Quantum Hall States in Bilayer Graphene*, *Science* **358**, 648 (2017).
- [19] G. Diankov, C.-T. Liang, F. Amet, P. Gallagher, M. Lee, A. J. Bestwick, K. Tharratt, W. Coniglio, J. Jaroszynski, K. Watanabe *et al.*, *Robust Fractional Quantum Hall Effect in the  $n = 2$  Landau Level in Bilayer Graphene*, *Nat. Commun.* **7**, 13908 (2016).
- [20] S. Kivelson, *Semiclassical Theory of Localized Many-Anyon States*, *Phys. Rev. Lett.* **65**, 3369 (1990).
- [21] F. D. M. Haldane, "Fractional Statistics" in Arbitrary Dimensions: A Generalization of the Pauli Principle, *Phys. Rev. Lett.* **67**, 937 (1991).
- [22] M. V. N. Murthy and R. Shankar, *Haldane Exclusion Statistics and Second Virial Coefficient*, *Phys. Rev. Lett.* **72**, 3629 (1994).
- [23] V. Venkatachalam, A. Yacoby, L. Pfeiffer, and K. West, *Local Charge of the  $\nu = 5/2$  Fractional Quantum Hall State*, *Nature (London)* **469**, 185 (2011).
- [24] Z. Papić, R. Thomale, and D. A. Abanin, *Tunable Electron Interactions and Fractional Quantum Hall States in Graphene*, *Phys. Rev. Lett.* **107**, 176602 (2011).
- [25] Z.-X. Hu, R. N. Bhatt, X. Wan, and K. Yang, *Realizing Universal Edge Properties in Graphene Fractional Quantum Hall Liquids*, *Phys. Rev. Lett.* **107**, 236806 (2011).
- [26] D. Wong, J. Velasco, L. Ju, J. Lee, S. Kahn, H.-Z. Tsai, C. Germany, T. Taniguchi, K. Watanabe, A. Zettl, F. Wang, and M. F. Crommie, *Characterization and Manipulation of Individual Defects in Insulating Hexagonal Boron Nitride Using Scanning Tunneling Microscopy*, *Nat. Nanotechnol.* **10**, 949 (2015).
- [27] R. B. Laughlin, *Anomalous Quantum Hall Effect: An Incompressible Quantum Fluid with Fractionally Charged Excitations*, *Phys. Rev. Lett.* **50**, 1395 (1983).
- [28] J. K. Jain, *Composite-Fermion Approach for the Fractional Quantum Hall Effect*, *Phys. Rev. Lett.* **63**, 199 (1989).
- [29] F. D. M. Haldane, *Fractional Quantization of the Hall Effect: A Hierarchy of Incompressible Quantum Fluid States*, *Phys. Rev. Lett.* **51**, 605 (1983).
- [30] K. R. Patton and M. R. Geller, *Fractionally Charged Impurity States of a Fractional Quantum Hall System*, *New J. Phys.* **16**, 023004 (2014).
- [31] See Supplemental Material at <http://link.aps.org/supplemental/10.1103/PhysRevX.8.011037> for details, which includes Refs. [32,33].
- [32] E. Prodan and F. D. M. Haldane, *Mapping the Braiding Properties of the Moore-Read State*, *Phys. Rev. B* **80**, 115121 (2009).
- [33] N. Read and E. Rezayi, *Beyond Paired Quantum Hall States: Parafermions and Incompressible States in the First Excited Landau Level*, *Phys. Rev. B* **59**, 8084 (1999).

- [34] R. E. Prange and S. M. Girvin, *The Quantum Hall Effect, Graduate Texts in Contemporary Physics* (Springer-Verlag, Berlin, 1987).
- [35] Indeed, guiding-center dynamics imply that the quadrupole moment and angular momentum of an excitation are related by  $Q_{zz} = e\ell_B^2 L^z / \hbar$ .
- [36] R. E. Prange, *Quantized Hall Resistance and the Measurement of the Fine-Structure Constant*, *Phys. Rev. B* **23**, 4802 (1981).
- [37] J. K. Jain and M. R. Peterson, *Reconstructing the Electron in a Fractionalized Quantum Fluid*, *Phys. Rev. Lett.* **94**, 186808 (2005).
- [38] B. A. Bernevig and F. D. M. Haldane, *Model Fractional Quantum Hall States and Jack Polynomials*, *Phys. Rev. Lett.* **100**, 246802 (2008).
- [39] G. Moore and N. Read, *Nonabelions in the Fractional Quantum Hall Effect*, *Nucl. Phys.* **B360**, 362–396 (1991).
- [40] A. Sterdyniak, N. Regnault, and B. A. Bernevig, *Extracting Excitations from Model State Entanglement*, *Phys. Rev. Lett.* **106**, 100405 (2011).
- [41] M. Levin, B. I. Halperin, and B. Rosenow, *Particle-Hole Symmetry and the Pfaffian State*, *Phys. Rev. Lett.* **99**, 236806 (2007).
- [42] S.-S. Lee, S. Ryu, C. Nayak, and M. P. A. Fisher, *Particle-Hole Symmetry and the  $\nu = \frac{5}{2}$  Quantum Hall State*, *Phys. Rev. Lett.* **99**, 236807 (2007).
- [43] D. T. Son, *Is the Composite Fermion a Dirac Particle?*, *Phys. Rev. X* **5**, 031027 (2015).
- [44] P. T. Zucker and D. E. Feldman, *Stabilization of the Particle-Hole Pfaffian Order by Landau-Level Mixing and Impurities that Break Particle-Hole Symmetry*, *Phys. Rev. Lett.* **117**, 096802 (2016).
- [45] R. Willett, J. P. Eisenstein, H. L. Störmer, D. C. Tsui, A. C. Gossard, and J. H. English, *Observation of an Even-Denominator Quantum Number in the Fractional Quantum Hall Effect*, *Phys. Rev. Lett.* **59**, 1776 (1987).
- [46] T. H. Hansson, M. Hermanns, N. Regnault, and S. Viefers, *Conformal Field Theory Approach to Abelian and Non-Abelian Quantum Hall Quasielectrons*, *Phys. Rev. Lett.* **102**, 166805 (2009).
- [47] B. A. Bernevig and F. D. M. Haldane, *Clustering Properties and Model Wave Functions for Non-Abelian Fractional Quantum Hall Quasielectrons*, *Phys. Rev. Lett.* **102**, 066802 (2009).
- [48] Ivan D. Rodriguez, A. Sterdyniak, M. Hermanns, J. K. Slingerland, and N. Regnault, *Quasiparticles and Excitons for the Pfaffian Quantum Hall State*, *Phys. Rev. B* **85**, 035128 (2012).
- [49] K. Ichimura, M. Osawa, K. Nomura, H. Kataura, Y. Maniwa, S. Suzuki, and Y. Achiba, *Tunneling Spectroscopy on Carbon Nanotubes Using STM*, *Physica (Amsterdam)* **323B**, 230 (2002).
- [50] L. S. Levitov and A. M. Tsvetlik, *Narrow-Gap Luttinger Liquid in Carbon Nanotubes*, *Phys. Rev. Lett.* **90**, 016401 (2003).
- [51] M. Ruby, F. Pientka, Y. Peng, F. von Oppen, B. W. Heinrich, and K. J. Franke, *Tunneling Processes into Localized Subgap States in Superconductors*, *Phys. Rev. Lett.* **115**, 087001 (2015).
- [52] J. P. Eisenstein, T. Khaire, D. Nandi, A. D. K. Finck, L. N. Pfeiffer, and K. W. West, *Spin and the Coulomb Gap in the Half-Filled Lowest Landau Level*, *Phys. Rev. B* **94**, 125409 (2016).
- [53] J. Jang, B. M. Hunt, L. N. Pfeiffer, K. W. West, and R. C. Ashoori, *Sharp Tunneling Resonance from the Vibrations of an Electronic Wigner Crystal*, *Nat. Phys.* **13**, 340 (2017).
- [54] Y. Zhang, J. K. Jain, and J. P. Eisenstein, *Tunnel Transport and Interlayer Excitons in Bilayer Fractional Quantum Hall Systems*, *Phys. Rev. B* **95**, 195105 (2017).
- [55] J. Jang, H. M. Yoo, L. Pfeiffer, K. West, K. W. Baldwin, and R. Ashoori, *Full Momentum and Energy Resolved Spectral Function of a 2D Electronic System*, *Science* **358**, 901 (2017).
- [56] M. Barkeshli, P. Bonderson, M. Cheng, and Z. Wang, *Symmetry, Defects, and Gauging of Topological Phases*, arXiv:1410.4540.